Sla1p couples the yeast endocytic machinery to proteins regulating actin dynamics

Derek T. Warren[1], Paul D. Andrews[2], Campbell W. Gourlay[1] and Kathryn R. Ayscough[1,*]

[1]Institute of Biomedical and Life Sciences, Division of Biochemistry and Molecular Biology, University of Glasgow, Glasgow. G12 8QQ, UK
[2]Wellcome Trust Biocentre, Division of Molecular Cell Biology, School of Life Sciences, University of Dundee, Dow Street, Dundee, DD1 5EH, UK
Author for correspondence (e-mail: k.ayscough@bio.gla.ac.uk)

Accepted 17 January 2002
Journal of Cell Science 115, 1703-1715 (2002) © The Company of Biologists Ltd

Summary

Sla1p is a protein required for cortical actin patch structure and organisation in budding yeast. Here we use a combination of immunofluorescence microscopy and biochemical approaches to demonstrate interactions of Sla1p both with proteins regulating actin dynamics and with proteins required for endocytosis. Using Sla1p-binding studies we reveal association of Sla1p with two proteins known to be important for activation of the Arp2/3 complex in yeast, Abp1p and the yeast WASP homologue Las17p/Bee1p. A recent report of Sla1p association with Pan1p puts Sla1p in the currently unique position of being the only yeast protein known to interact with all three known Arp2/3-activating proteins in yeast. Localisation of Sla1p at the cell cortex is, however, dependent on the EH-domain-containing protein End3p, which is part of the yeast endocytic machinery. Using spectral variants of GFP on Sla1p (YFP) and on Abp1p (CFP) we show for the first time that these proteins can exist in discrete complexes at the cell cortex. However, the detection of a significant FRET signal means that these proteins also come close together in a single complex, and it is in this larger complex that we propose that Sla1p binding to Abp1p and Las17p/Bee1p is able to link actin dynamics to the endocytic machinery. Finally, we demonstrate marked defects in both fluid-phase and receptor-mediated endocytosis in cells that do not express *SLA1*, indicating that Sla1p is central to the requirement in yeast to couple endocytosis with the actin cytoskeleton.

Key words: Actin, *Saccharomyces cerevisiae*, Endocytosis, SH3-domain, EH-domain

Introduction

In yeast, the actin cytoskeleton comprises two types of structure that are visible by fluorescence microscopy. Actin patches are punctate structures, containing F-actin, that localise to the cell cortex, whereas actin cables are elongated structures that are found running through the cytoplasm of cells (Adams and Pringle, 1984). Studies using a combination of mutational approaches and actin-disrupting drugs have revealed the importance of the yeast actin cytoskeleton for polarised cell growth, organelle inheritance and endocytosis (Novick and Botstein, 1985; Kübler and Riezman, 1993; Ayscough et al., 1997; Simon et al., 1997). However, the mechanisms underlying the observed involvement of the actin cytoskeleton in these essential cell processes and the precise functional contributions made by the patch and cable structures remain poorly understood. Live cell imaging of cortical patches using GFP-tagged actin or the actin-binding proteins Abp1p and Cap2p has demonstrated that these patches can be highly motile at the cell cortex, with velocities of up to 0.5 μm/sec (Doyle and Botstein, 1996; Waddle et al., 1996). However, cortical actin patches have also been suggested to associate with sites of endocytosis (Mulholland et al., 1994), which would seem less likely to be motile. To date it has been difficult to reconcile these apparently conflicting observations.

As with the actin cytoskeleton of other eukaryotic cells, the actin patches and cables of budding yeast are not composed of F-actin alone. Many proteins associate with actin to regulate its dynamic properties and allow it to reorganise in response to both internal and external cues. Several proteins (e.g. Abp1p, Sac6p and cofilin) are known to bind directly to actin and alter its dynamic properties. Other proteins have been reported to localise to polarised sites of active cell growth but have not been demonstrated to bind to actin directly. Deletion of the genes encoding some of these proteins can have dramatic effects on the organisation and structure of the cortical actin cytoskeleton, suggesting that some proteins can regulate the cortical actin cytoskeleton but are not always tightly associated with it.

The studies reported here focus on the role of a protein Sla1p, which was originally identified through a synthetic lethal genetic screen to isolate mutants that required the expression of a gene *ABP1* (actin-binding protein 1) (Holtzman et al., 1993). Further studies demonstrated that Sla1p is a multifunctional protein required for cortical actin patch structure and organisation in budding yeast (Ayscough et al., 1999). Sla1p has three SH3 domains in its N-terminal third and a C-terminal domain comprising multiple repeats rich in proline, glutamine, glycine and threonine. This repeat domain has recently been shown, by immunoprecipitation, to interact with the N-terminal EH-domain of End3p and the LR1 domain of Pan1p (Tang et al., 2000). End3p and Pan1p are EH-domain-containing proteins shown in several studies to be required for endocytosis in yeast and, when their genes are disrupted, to cause aberrant effects on the actin cytoskeleton (Raths et al., 1993; Benedetti et al., 1994; Tang and Cai, 1996; Tang et al., 1997; Wendland and Emr, 1998). EH-domain-containing

Table 1. Yeast strains used in this study

KAY#	Genotype	Origin/reference
415	MAT**a** *leu2, trp1, ura3-52, prb1-1122, pep4-3, prc1-451*	D. Drubin (UC Berkeley) (DDY1810)
419	KAY415 + pJC230 (GST-SLA1)	
302	MATα, *trp1-1, leu2-3,112, lys2-801, his3-Δ200, ura3-52*	D. Drubin (UC Berkeley)
404	KAY302 + integrated SLA1-YFP::HIS3	This study
389	MAT**a**, *trp1-1, leu2-3,112, his3-Δ200, ura3-52*	This study
425	KAY389 + *ABP1-CFP::KanMx*	This study
441	MAT**a** *trp1-1, leu2-3,112, his3-Δ200, ura3-52, ABP1-CFP::KanMx, SLA1-YFP::HIS3*	This study
442	KAY441 x KAY404	This study
397	KAY302 + integrated *SLA1-GFP::HIS3*	This study
400	KAY389 + integrated *SLA1-GFP::HIS3*	This study
401	KAY397 x KAY400	This study
303	KAY302 + *SLA1-9xmyc::TRP1*	This study
363	KAY302 + integrated *sla1ΔCt-9xmyc::TRP1*	This study
300	MAT**a**, *trp1-1, leu2-3,112, his3Δ200, ura3-52, Δsla1::URA3*	D. Drubin (UC Berkeley) (DDY958)
116	MAT**a**, *leu2-3,112, his3Δ200, ura3-52, bar1-1*	H. Riezman (Basel, Switzerland) (RH144-5D)
117	KAY116 + integrated *end3-1*	H. Riezman (Basel, Switzerland) (RH266-1D)
462	MAT**a**, *end3-1, leu2-3,112, his3Δ200, ura3-52, SLA1-GFP::HIS*	This study (117×397 segregant)
355	MATα, *trp1-1, leu2-3,112, lys2-801, his3-Δ200, ura3-52, Sla1*-3xHA::*TRP1*	This study
40	**a**/α *ura3-52/ura3-52*	This study
20	**a**/α *ura3-52/ura3-52 leu2-3,112/ leu2-3,112, his3-Δ200/ his3-Δ200, lys2-801/lys2-801, Δsla1::LEU2/Δsla1::LEU2*	This study
451	MAT**a** *Δend3::KanMx, ura3Δ, leu2Δ, lys2Δ, his3Δ*	Research Genetics
517	MATα *Δend3::KanMx, ura3Δ, leu2Δ, lys2Δ, his3Δ Sla1GFP::HIS3*	This study (451×397 segregant)
316	MAT**a**, *ura3-52, lys2-801, ade2-101, trp1-Δ63, his3-Δ200, leu2-Δ1, pFUS1-LACZ::URA3, Ste2-myc::TRP1*	Ayscough and Drubin, 1998
391	MAT**a**, *ura3-52, lys2-801, ade2-101, trp1-Δ63, his3-Δ200, leu2-Δ1, pFUS1-LACZ::URA3, Ste2-myc::TRP1, Δsla1::LEU2*	This study

Table 2. Plasmids used in this study

Plasmid	Description	Origin
pJC230	pEG-KT, *URA3*, *LEU2*, *GST-SLA1*	J. Cope and D. Drubin (UC Berkeley).
pWZV87	For C-terminal 9×myc tagging (TRP marked)	K. Nasmyth (IMP, Vienna)
PWZV86	For TRP marked gene deletions	K. Nasmyth (IMP, Vienna)
pWZV89	For C-terminal HA tagging (HIS marked)	K. Nasmyth (IMP, Vienna)
pFA6a-GFP(S65T)::HIS3MX6	For C-terminal GFP tagging (HIS marked)	(Longtine et al., 1998)
pDH5	For C-terminal YFP tagging (HIS marked)	Yeast Resource Centre, University of Washington
pDH3	For C-terminal CFP tagging (HIS marked)	Yeast Resource Centre, University of Washington
pAbp1-GFP	GFP tagged Abp1p	T. Doyle, D. Botstein (Stanford University)

proteins in mammalian cells, including the Pan1p homologue Eps15, localise to clathrin-coated pits and are involved in endocytic events (Tebar et al., 1996). In yeast, endocytosis has been demonstrated, by several approaches, to require a functional actin cytoskeleton. These approaches include analysis of mutant phenotypes, biochemical studies of specific protein-protein interactions within endocytic complexes and the addition of actin-disrupting drugs such as latrunculin-A and jasplakinolide (Kübler and Riezman, 1993; Ayscough et al., 1997; Wesp et al., 1997; Ayscough, 2000). The situation in mammalian cells is more contentious. Despite reports showing interactions between the actin cytoskeleton and clathrin, and data showing rearrangements of cortical actin in response to overexpression of certain endocytic proteins, the links between the processes have not been well enough defined to be generally accepted (for a review, see Geli and Riezman, 1998). A potential reason for the lack of a clearly defined link is that the coupling of the processes is highly dynamic and possibly involves interactions between separate protein complexes depending on the nature of the cargo being internalised.

The studies we present demonstrate that Sla1p localises to the cell cortex through interactions with proteins of the endocytic machinery. However, we also demonstrate that Sla1p binds to proteins involved in regulating actin dynamics. We propose that Sla1p plays a central role in coupling the endocytic machinery to the actin cytoskeleton and that this link allows activation of proteins that can promote actin polymerisation. This coupling is necessary in order for cells to undergo normal levels of both fluid-phase and receptor-mediated endocytosis.

Materials and Methods

Materials

The chemicals used were obtained from BDH/Merck unless otherwise stated. Media was from Melford Laboratories (yeast extract, peptone and agar) or Sigma (minimal synthetic medium and amino acids). Latrunculin-A was a gift from Phil Crews (UC Santa Cruz).

Yeast strains and cell growth

The yeast strains used in this study are listed in Table 1. The plasmids and oligonucleotides used to generate PCR products for direct deletions and epitope tagging of the genomic copies of genes are given in Table 2 and Table 3. Unless otherwise stated, yeast cells were grown with rotary shaking at 30°C in liquid YPD medium (1% yeast extract, 2 Bacto-peptone, 2% glucose supplemented with 40 μg/ml

Table 3. Oligonucleotides used in this study

Oligo	Sequence	Description
oKA7	CCTCAACAATCAAGGCAAGCCAACATATTCAATGCTACTGCATCAAATCC-GTTTGGATTCTCCGGTTCTGCTGCTAG	C-terminal Myc and HA tagging SLA1 (5′)
oKA8	ACGAAACTATTTCATATATCGTGTTTTAGTTATTATCCTATAAAATCTTAAAA-TACATTAATCCCTCGAGGCCAGAAGAC	C-terminal Myc and HA tagging SLA1 (3′)
oKA78	TGCTGCTCCGGTTTCATCTGCTCCGGTTTCATCTGCTCCCGCTCCATTGG-ATCCATTCAATCCGGTTCTGCTGCTAG	Myc tagging and deleting C- terminal repeats of SLA1 (5′)
oKA79	GTAATCATTGGCATCATCACAAAGCCAGTAGATAAGGGTAAGATATTGTT-GCCACCGGTTCCTCGAGGCCAGAAGAC	Myc tagging and deleting C-terminal repeats of SLA1 (3′)
oKA132	CTCAACAATCAAGGCAAGCCAACATATTCAATGCTACTGCATCAAATCCG-TTTGGATTCGCTGCAGCCGCTGCAGCTGCACGGATCCCCGGGTTAATTAA	GFP/YFP tag on C-terminus of SLA1 + 7×Ala linker (5′)
oKA133	ACGAAACTATTTCATATATCGTGTTTTAGTTATTATCCTATAAAATCTTAAAA-TACATTAATCGAATTCGAGCTCGTTTAAAC	GFP/YFP tag on C-terminus of SLA1 (3′)
oKA134	AAGACGGCTCAAAAGGTCTCTTCCCCAGCAATTATGTGTCTTTGGGCAA-CCGGATCCCCGGGTTAATT	CFP tag on Abp1 C terminus (5′)
oKA129	TACAAAAGCTTTAACGTCTCTGTAAGTATTTTTTTACGTAAGAATAATATAA-TAGCATGAGAATTCGAGCTCGTTTAAA	CFP tag on Abp1 C terminus (3′)

adenine). Tetrads were dissected using a Singer Instruments MSM Manual micromanipulator. Transformations were performed using lithium acetate as previously described (Kaiser et al., 1994).

Preparation of GST-Sla1p and Sla1p antibodies

A 4 l culture of KAY419 cells was induced to overexpress the GST-Sla1p fusion protein. Cells were grown to an OD (600 nm) of 1.0 in synthetic media lacking uracil and subcultured into the same media, which had 2% raffinose as the sole carbon source also to an OD (600 nm) of 1.0. Cells were then harvested and resuspended in twice the original volume of YPD plus 2% galactose, and GST-SLA1 expression was induced for 24 hours. Cells were harvested, washed and resuspended in an equal volume of 2× PBS containing protease inhibitors (0.5 mg/ml leupeptin, aprotinin, chymostatin, pepstatin A and 1 mM PMSF) before freezing in liquid nitrogen and then being broken using a bead beater (Biospec Products Inc.) The lysate was then spun at 2000 ***g*** for 4 minutes, the supernatant was removed and spun at 28000 ***g*** for 20 minutes. The resultant supernatant was spun at 100,000 ***g*** for 1 hour and the final supernatant removed to a clean tube. All centrifugation steps were carried out at 4°C. The final supernatant was passed through a DEAE-sepharose 4B matrix (Amersham Pharmacia Biotech) that had been equilibrated with PBS. After loading the sample, the column was washed with PBS to elute unbound proteins, and bound proteins were eluted in a 0-1.0 M KCl gradient (this stage is required to remove an unknown factor that inhibits GST-Sla1p binding to glutathione beads). Fractions containing GST-Sla1p were identified by immunoblotting and pooled before being incubated with glutathione sepharose 4B beads (Amersham Pharmacia Biotech); 1 ml of glutathione beads was used per 50 ml of GST-Sla1p-containing fractions. Purity was assessed on coomassie-stained SDS polyacrylamide gels; multiple bands were observed as Sla1p is readily broken down cells when overexpressed, but all bands present were detected on immunoblots with an anti-GST antibody.

Polyclonal rabbit antisera were raised against purified GST-Sla1p protein. Four injections of approximately 50 μg of protein were administered to two New Zealand White rabbits at 28 day intervals (Diagnostics Scotland). Bleeds were carried out 7 days after each injection. Polyclonal antibodies were affinity purified from bleed four antisera. GST-Sla1p (250 μg) was coupled to 1 g of activated CNBr beads (Amersham Pharmacia Biotech). 2 ml of bleed four antisera were passed over a column of GST-Sla1p bound CNBr beads six times. The column was washed and antisera eluted first with 100 mM glycine, pH 2.5, (neutralised with 10 mM Tris-HCl, pH 7.5) and then with 100 mM triethylamine. pH 11.3. Fractions collected were neutralised with 1 M Tris-HCl, pH 8.0 and analysed for protein content by spectophotometry at an OD of 280 nm. The affinity-purified antisera obtained from the basic elution recognised purified GST-Sla1p but not purified GST by western blotting (data not shown) and gave rise to a band of the expected size (approximately 175 kDa) in wild-type cell protein extracts that was not present in sla1-null cells.

GST-Sla1p pull-down assays and immunoprecipitations

Pull-down assays were carried out with purified GST-Sla1p bound to glutathione sepharose 4B beads. A 20 ml culture of KAY419 was grown to mid-log phase in synthetic media lacking uracil. Cells were harvested, washed twice in binding buffer (50 mM HEPES, 100 mM KCl, 1 mM EGTA, 1 mM EDTA, 0.5% deoxycholic acid, 1 mM PMSF and 1× aqueous protease inhibitor mix) before resuspending in 2 ml of binding buffer. Whole cell lysates were prepared by the liquid nitrogen grinding method as previously described (Sorger and Pelham, 1987). Lysates were spun at 2000 ***g*** for 4 minutes to remove unbroken cells and the supernatant spun at 300,000 ***g*** for 20 minutes; both centrifugation steps were at 4°C. The final supernatant was removed and 100 μl incubated with either 20 μl of GST-Sla1p-coated glutathione beads or with 20 μl of pre-equilibrated glutathione sepharose for 3 hours at 4°C with rotation. The beads were pelleted at 500 ***g*** for 4 minutes and washed three times in 10 bed volumes of binding buffer. Bound proteins were eluted in sample buffer and separated on a 10% SDS polyacrylamide gel before transfer to PVDF for analysis.

Immunoprecipitations were performed essentially as described by Li (Li, 1997). Yeast cells were lysed by grinding in liquid nitrogen in 2×UBT (100 mM KHepes, pH 7.5, 200 mM KCl, 6 mM $MgCl_2$, 2 mM EGTA, 1% Triton X-100) freshly supplemented with protease inhibitors. The cell lysate was centrifuged at 100,000 ***g*** for 20 minutes. 40 μl of high-speed extract was incubated for 1 hour at 4°C with 20 μl protein A-Sepharose beads (Pharmacia) with rabbit anti-Abp1p polyclonal antibody bound (a gift from D. Drubin) or with rabbit anti-myc polyclonal antibody bound as the control (Sigma). The beads were washed three times in 2×UBT buffer, and bound proteins were eluted by boiling in 4×SDS sample buffer for 1 minute. 10 μl of cell extract, 10 μl of the final wash and10 μl of eluted proteins were loaded onto a 10% polyacrylamide gel before transfer to PVDF for analysis by western blotting.

Internalisation assays with radiolabelled pheromone

The internalisation assays were performed using a modified α-factor pheromone peptide that can be iodinated. This peptide (MFN5) has been characterised and elicits the same biological responses in budding yeast as the unmodified α-factor pheromone (Siegel et al., 1999). The MFN5 peptide was iodinated with chloramine T as described in Olah et al. and Siegel et al. (Olah et al., 1994; Siegel et

al., 1999). For the assay, YPAD plates were spread with 200 μl (2×10^6 cells) from an overnight culture of either KAY316 or KAY391 cells. Plates were incubated overnight at 30°C. Cells were resuspended in YPAD + 1M sorbitol and centrifuged at 500 rpm for 5 minutes. The supernatant was decanted into a fresh tube, and cells were harvested by centrifugation. Cells was resuspended in ice cold YPAD to a concentration of 5×10^8 cells/ml. α-factor internalistion assays were performed essentially as described previously (Dulic et al., 1991). ^{125}I-MFN5 peptide was allowed to bind to cells on ice. Unbound MFN5 peptide was removed by centrifugation and cells were resuspended in pre-warmed (30°C) YPAD media to initiate peptide internalisation. At various time points, cell aliquots were removed and washed in pH 1.1 or pH 6 buffer. The amount of cell-associated radioactivity after each wash was determined by gamma counting in a COBRA™ Auto-Gamma counter (PACKARD). The amount of α-factor peptide internalised is calculated as a ratio of pH-1.1-resistant to pH-6-resistant radioactivity.

Fluorescence microscopy procedures

Endocytosis of the fluid-phase marker lucifer yellow was performed according to the method of Dulic and colleagues (Dulic et al., 1991). Quantitation of fluorescence intensity for staining vacuoles was performed using IP lab™ software. Rhodamine-phalloidin (Molecular Probes) staining was performed as described previously (Hagan and Ayscough, 2000). Cells were processed for immunofluorescence essentially as described by Ayscough and Drubin (Ayscough and Drubin, 1998a). Following fixation with formaldehyde, cells adhered to slides with poly-L-lysine and were treated for 1 minute with 0.1% SDS in PBS before incubating with antibodies. Primary antibodies used in this study were A14 anti-myc at a dilution of 1:100 (Santa Cruz Biotechnology Inc.) and anti-yeast actin used at 1:1000 (a gift from David Drubin, UC Berkeley). Secondary antibodies used were fluorescein-isothiocyanate (FITC)-conjugated goat anti-guinea-pig (Cappell/Organon) at a dilution of 1:1000 and CY3-conjugated sheep anti-rabbit (Sigma Chemical Co., Poole, UK) at a dilution of 1:200. Cells were viewed with an Olympus BX-60 fluorescence microscope with a 100 W mercury lamp and an Olympus 100× Plan-NeoFluar oil-immersion objective. Images were captured using a Roper Scientific MicroMax 1401E cooled CCD camera using Scanalytics IP lab software on an Apple Macintosh 7300 computer.

Fluorescently tagged strains were made by integration of PCR-generated DNA fragments onto the genomic sequences of the appropriate genes as described by Longtine and colleagues (Longtine et al., 1998). Tags were inserted at the sequence corresponding to the C-terminus of Abp1p and at the C-terminus of Sla1p following insertion of a seven alanine linker. Cells expressing CFP-tagged Abp1p and YFP-tagged Sla1p (KAY441) or GFP-tagged Sla1p (KAY397, KAY462) were visualised after growing to log phase in suspension in YPD media supplemented with adenine or after being taken from a freshly growing colony on a plate. For imaging, 3 μl of cells were put on a slide, covered with a coverslip and sealed with nail polish. For single images of Sla1-GFP cells, cells were viewed and images recorded as described above.

For timelapse live cell imaging, exponentially growing cells were harvested and resuspended in a smaller volume of synthetic complete medium containing glucose (SCD) and then applied to a slide to which a thin pad of 25% gelatin (Porcine 300 bloom; Sigma, UK) in SCD had been applied. After sealing with a coverslip and rubber cement, cells were imaged for YFP and CFP or GFP alone. Imaging of CFP and YFP fusion proteins co-expressed in the same cell was performed using a DeltaVision Restoration Microscope System (Applied Precision Inc., Issaquah, WA USA), equipped with a Nikon Plan Apo 100× (1.4 NA) objective and a Roper Scientific Interline Cooled CCD camera (5 MHz MicroMax1300YHS) utilising the JP4 filter set (CFP excitation 436/10; CFP emission 470/30; YFP excitation 500/14; YFP emission 535/30; dichroic JP4 beamsplitter; Chroma Inc, USA). Optical sectioning was performed at 0.4 μm intervals to encompass the entire cell, limiting exposure times to 0.09 seconds. Data were collected in fast acquisition mode, imaging both wavelengths before changing the Z position. 3D image data sets were deconvolved using the SoftWoRx application (Applied Precision Inc., USA) running on a Silicon Graphics Octane workstation (Silicon Graphics Inc., USA). 2D maximum-intensity projections were generated from the 3D datasets using SoftWoRx and images captured in TIFF format using MediaRecorder (Silicon Graphics Inc., USA) and assembled using Adobe PhotoShop (Adobe Inc., USA).

FRET analysis

To measure fluorescence resonance energy transfer (FRET), cells were prepared and mounted as above, and single images corresponding to the middle optical section were acquired using the DeltaVision microscope. Images were always taken in the same order using the following JP4 filter set combinations: 'YFP' (Ex:YFP/EM:YFP), 'CFP' (Ex:CFP/EM:CFP), 'FRET'(Ex:CFP/Em:YFP), 'FRET control' (Ex:YFP/Em:CFP). Excitation and emission filter wheels and shutters were automatically controlled using the SoftWoRx software. 2×2 binning was used to increase signal-to-noise ratios. Exposures times were 800 mseconds throughout to give a signal in the mid-high range of the CCD camera. Some of the complexes being imaged in live cells were seen to move slightly during the course of data collection, resulting in a small shift between wavelengths in the merged images. Quantitation of corrected FRET was performed on a pixel-by-pixel basis essentially as described previously (Sorkin et al., 2000; Gordon et al., 1998). Cross-over between donor (CFP) and acceptor (YFP) fluorescence via the FRET filter was calculated as a constant proportion of the donor and acceptor fluorescence through the donor and acceptor filters and is a function of these particular filter sets. For the DeltaVision system, the calculated mean ratio for the donor was 0.58 and for the acceptor was 0.30. Corrected FRET ($FRET^C$) was therefore calculated as: $FRET^C$='FRET'–(0.58×'CFP')–(0.3×'YFP'). Images were processed using the ImageArithmetic function within SoftWoRx. The final $FRET^C$ image was displayed with a pseudocoloured scale representing arbitary units of fluorescence intensity and as a 3D histogram using the DataInspector function within SoftWoRx.

Results

Sla1p binds proteins involved in actin dynamics

Deletion of *SLA1* from yeast cells generates a phenotype in which the actin cytoskeleton is aberrant. Rather than many small polarised actin patches, the actin is found in larger, less well polarised 'chunks', although these are still localised to the cell cortex. Such a phenotype indicates that Sla1p is potentially involved in the dynamic turnover of actin filaments. Moreover, one report has shown that the yeast homologue of WASP, Las17p/Bee1p, can immunoprecipitate with Sla1p (Li, 1997). We decided to investigate the interaction with the actin cytoskeleton further by assessing binding of proteins to Sla1p.

Sla1p was purified as a GST fusion from yeast cells as described in Materials and Methods. Wild-type cell extracts were incubated with either GST-Sla1p beads or with GST beads alone. Following extensive washing, the proteins associated with the beads were separated by SDS-PAGE and transferred to PVDF membranes. Western blotting revealed binding of Abp1p and Las17p/Bee1p with the GST-Sla1p beads, whereas other proteins, including Sac6p, cofilin, Arp2p

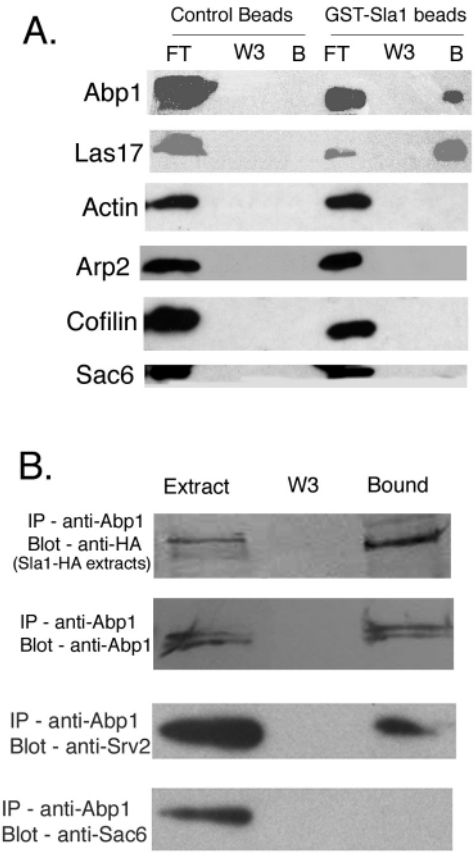

Fig. 1. Interaction of Sla1p with proteins involved in actin dynamics. (A) GST-Sla1p was overexpressed in yeast as described in Materials and Methods and purified on glutathione sepharose beads following ion exchange chromatography. Yeast extracts were incubated with either GST-Sla1p beads or with glutathione beads alone. Beads were spun down, washed and bound proteins eluted in SDS sample buffer. Analysis was by western blotting using antibodies as marked. (Lanes: FT, flow through; W3, third wash; B, bound). (B) Further evidence of the Sla1p-Abp1 interaction was demonstrated using immunoprecipitation. Yeast cell extracts from a strain expressing Sla1-HA (KAY355) were incubated with protein-A sepharose bound with anti-Abp1p antibodies. After washing, the bound proteins were separated by SDS-PAGE and transferred to PVDF. The blot was probed with antibodies to Abp1p or HA to detect Sla1p, Srv2p and Sac6p. E, extract; W3, third wash; B, bound.

and actin, did not bind to the Sla1p beads (Fig. 1A). None of the proteins bound to the control beads alone.

Although an interaction between Sla1p and Las17p/Bee1p had been previously shown using an immunoprecipitation approach (Li, 1997), the Sla1p-Abp1p physical interaction has not been identified in other studies. To verify this interaction, antibodies to Abp1p were used to immunoprecipitate HA-tagged Sla1p from wild-type cell extracts (Fig. 1B). Srv2p, a previously known Abp1p interactor, (Lila and Drubin, 1997) also coimmunoprecipitates, whereas Sac6p, an actin bundling protein, does not coimmunoprecipitate with Abp1p.

Cells lacking Sla1p are significantly more resistant to the effects of the actin-disrupting drug latrunculin-A

Latrunculin-A (LAT-A) binds across the nucleotide-binding cleft of monomeric actin in cells and prevents reincorporation of that actin into filaments (Ayscough et al., 1997; Morton et al., 2000). Wild-type yeast cells are sensitive to the effects of LAT-A despite having only very low levels of G-actin (Karpova et al., 1995), indicating that their actin cytoskeleton is dynamic. In a previous report, using a halo assay test, we demonstrated an enhanced LAT-A resistance of several mutant strains including cells lacking Sla1p (Ayscough et al., 1997). To explore this further, we analysed the LAT-A sensitivity of Δ*sla1* cells in more detail. We added LAT-A of concentrations up to 1 mM for 15 minutes and used rhodamine-phalloidin staining to visualise the actin cytoskeleton. In control cells (*SLA1*), the percentage of cells containing cortical actin patches was less than 5% following addition of 200 μM LAT-A, and at 1 mM LAT-A, no F-actin structures were seen at all. In contrast, cells that did not express *sla1* (Δ*sla1*) were dramatically more resistant to LAT-A effects, and the majority of cells still contained cortical actin structures after incubation with 1 mM LAT-A after 15 minutes (Fig. 2A). To address whether the resistance was caused by a kinetic delay in turnover of actin patches, wild-type and Δ*sla1* cells were incubated with 200 μM LAT-A for up to an hour. By 5 minutes, less than 10% of control cells contained discernible actin patches. However, more than 70% of Δ*sla1* cells still contained cortical actin after 1 hour (Fig. 2B). Both approaches indicate that the cortical actin in Δ*sla1* cells is considerably less dynamic than the actin in wild-type cells.

Imaging of Sla1p- and Abp1p-containing complexes at the cortex in live cells

Earlier studies suggested that both Sla1p and Abp1p associate with actin at the cell cortex (Lila and Drubin, 1997). Like actin, both proteins show a cortical patch localisation that is polarised to the presumptive bud site in the bud of small and medium budded cells and to the mother bud neck in large budded cells (Ayscough et al., 1999). Abp1p binds directly to actin and shows clear colocalisation with the cortical actin patches, although not with actin cables (Drubin et al., 1988). Abp1p localisation was monitored in these studies, rather than directly observing actin localisation, because tagging of Abp1p does not appear to interfere with its function. Direct tagging of yeast actin with GFP on the other hand does not generate a protein that can complement deletion of the wild-type actin gene (Doyle and Botstein, 1996).

We tagged the genomic copies of both *SLA1* and *ABP1* with sequences encoding spectral variants of the green fluorescent protein (Sla1p-YFP; Abp1p-CFP). For both proteins the addition of the tag did not affect the levels of the protein expressed in cells compared with untagged forms of the proteins as assessed by western blotting nor were there any detectable phenotypes caused by the tagging in terms of actin organisation or temperature sensitivity (data not shown). The 3D localisation of Sla1p and Abp1p was assessed in live cells using Deltavision restoration microscopy. As shown in Fig. 3, the two proteins only exhibited partial colocalisation with around 30% of Sla1p-YFP spots colocalising with Abp1p-CFP spots. This is the first clear indication that Sla1p-containing cortical complexes can exist as discrete subpopulations that are distinct but partially overlapping with other cortical actin-complexes in the same cells.

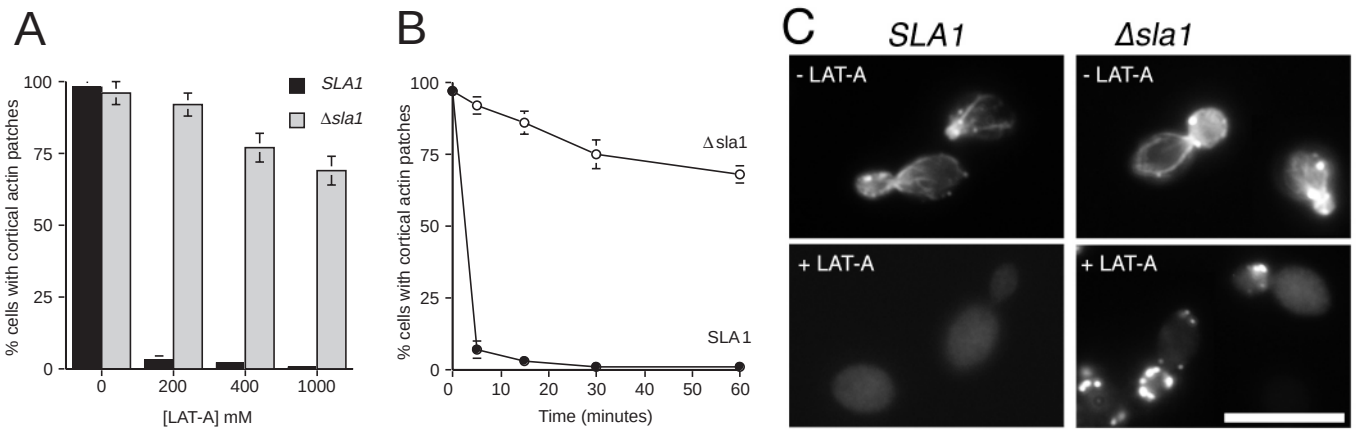

Fig. 2. The effect of *SLA1* deletion on sensitivity of cells to the actin disrupting drug latrunculin-A. KAY40 (*SLA1*) and KAY20 (Δ*sla1*) cells were grown to log phase at 30°C. (A) Cells were incubated with different concentrations of latrunculin-A (0-1000 μM) for 15 minutes before being fixed and processed for rhodamine-phalloidin staining. For each concentration of latrunculin-A, cells were counted to assess the percentage of cells that still contained cortical actin patches. (B) Cells were incubated with 200 μM latrunculin-A for up to 60 minutes. Samples were taken over this time period and fixed and processed for rhodamine-phalloidin staining. For each time point cells were counted to assess the percentage of cells that still contained cortical actin patches. Each experiment was repeated three times and 200-250 cells were counted for each concentration or time point on each occasion. The results plotted are the mean of these experiments. Error bars show standard errors of the mean. (C) Images showing wild-type and Δ*sla1* cells before and after treatment with 200 μM LAT-A for 1 hour. Note that although Δ*sla1* cells still contain punctate cortical structures they no longer contained visible actin cables after LAT-A treatment. Bar, 10 μM.

Fluorescence resonance energy transfer (FRET) analysis of Sla1p-Abp1p complexes

The partial overlap seen between Sla1p and Abp1 cortical populations suggests that although these proteins are often spatially separated they can and do associate in live cells. To address the question of colocalisation in more detail, we chose to use fluorescence resonance energy transfer (FRET), a technique that measures the non-radiative energy transfer between donor (e.g. CFP) and acceptor (e.g. YFP) molecules when they are in close proximity (less than 50Å). Hence, using FRET we aimed to determine whether or not colocalisation at the level of the light microscope correlates with a close association of Sla1p-YFP and Abp1-CFP in the context of a cortical protein complex. Digital images were acquired of optical sections at the middle of live cells through the CFP, YFP and FRET channels (Fig. 4A). Analysis of the raw FRET signals revealed high levels of fluorescence in the FRET channel in areas of the cortex where both Sla1p-YFP and Abp1-CFP were present and no FRET signal in areas where YFP and CFP signals were apart (Fig. 4A).

Corrected FRET ($FRET^C$) was calculated for the entire image on a pixel-by-pixel basis using a three-filter 'microFRET' method (Gordon et al., 1998; Sorkin et al., 2000). This correction eliminates intrinsic cross-over between donor and acceptor fluorescence through the FRET filter sets, which is a property of the optical system in use (see Materials and Methods for details). Significantly, this quantitative analysis of the true FRET signals reveals that the regions of the cortex where both Sla1p-YFP and Abp1-CFP are colocalised are indeed also the source of the very strong FRET signal (Fig. 4B). This leads to the conclusion that, although Abp1p and Sla1p are often found in separate parts of the cell cortex, when they do come together they do so in a protein complex that allows the two proteins to come within, at the most, 50Å of each other.

Movement of Sla1-GFP complexes at the cell cortex

Live cell imaging of cortical patches using GFP tagging of actin or of the actin binding proteins Abp1p and Cap2p has demonstrated that these patches can be highly motile at the cell cortex, with velocities of up to 0.5 μm/sec and with mean

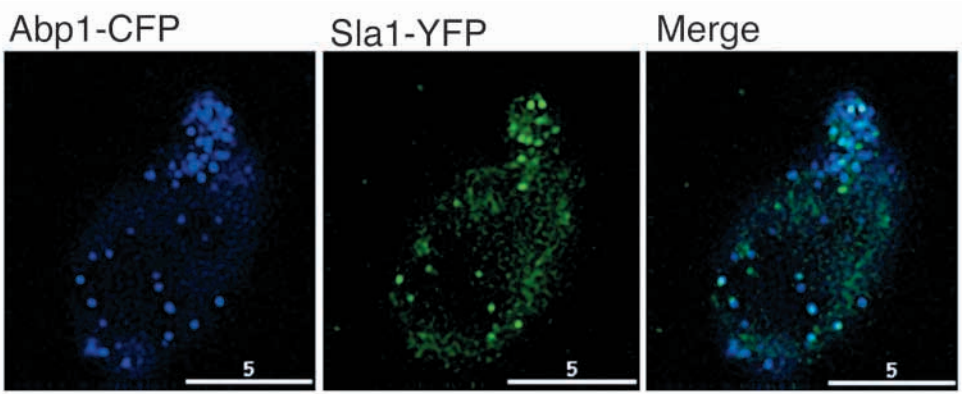

Fig. 3. Localisation of Sla1p-YFP and Abp1p-CFP in live cells. Exponentially growing KAY442 cells expressing Sla1p-YFP and Abp1p-CFP were mounted on gelatin slides and imaged using the JP4 filter set for YFP and CFP fluorescence. Images were recorded using the Deltavision Restoration microscope as described in the Materials and Methods. 2D maximum intensity projections of 3D data sets are shown.

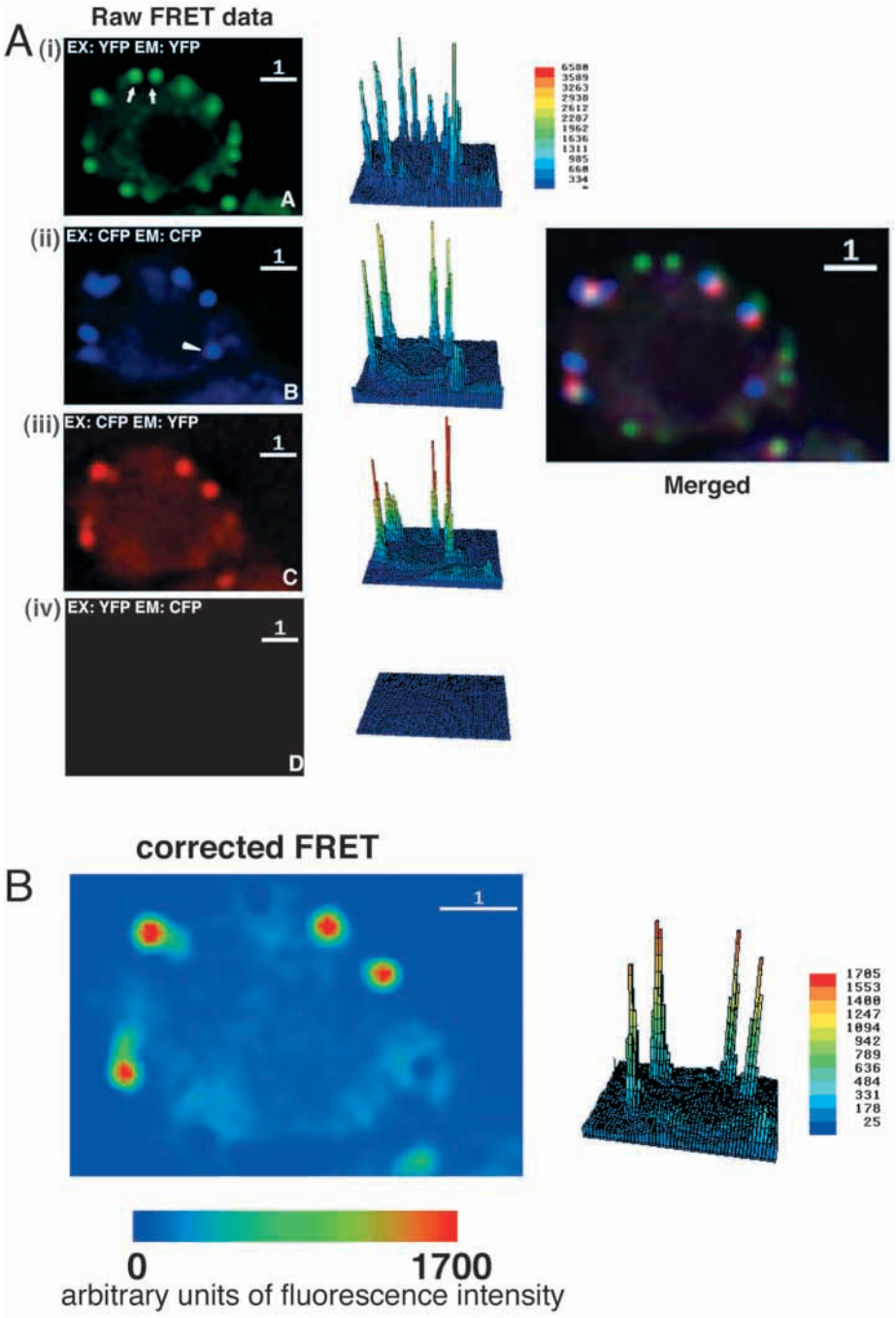

Fig. 4. FRET analysis of cells expressing Sla1p-YFP and Abp1p-CFP. FRET Images showing the interaction of Sla1p-YFP and Abp1p-CFP cortical patches. Fluorescence resonance energy transfer (FRET) between CFP and YFP was used to measure the relative proximity of Abp1 and Sla1p in KAY441 cells using the JP4 combination of excitation and emission filters sets and dichroic beamsplitter. (A) Deconvolved data from the FRET analysis showing (i) 'YFP' fluorescence, (ii) 'CFP' fluorescence, (iii) 'FRET' fluorescence and (iv) 'FRET control' fluorescence – zero in this case. Sla1p-YFP only populations (arrows), Abp1-CFP-only populations (arrowhead) and 'FRET' populations can be observed. 3D histograms of the data are shown to the right indicating the relative levels of the 'YFP', 'CFP' and 'FRET' signals in the raw data. The right hand panel shows a merged image showing the distinct overlapping populations. (B) The corrected FRET ($FRET^C$) image, after image arithmetic has been performed, is shown in quantitative pseudocolour representing arbitrary units of fluorescence intensity.

velocities measured from 0.06-0.3 μm/sec (Doyle and Botstein, 1996; Waddle et al., 1996; Belmont and Drubin, 1998). However, it is also notable that not all patches move with this velocity, and patches can change from fast movement to being almost static. To ascertain whether Sla1p shows movement comparable to that of the actin patches at the cell cortex, the localisation of Sla1-GFP was followed for various periods of time in living cells using high resolution, rapid image acquisition using the Deltavision microscope. A montage of this movement showing a deconvolved 3D image projected as a 2D image is shown in Fig. 5. Interestingly, in contrast to the high percentage of actin patches that move in cells, more than 90% of Sla1p-containing complexes appear to be static. The patches that were seen to move did so with a mean rate of 0.02 μm/second, which is significantly slower than the rate of actin patch movement, which in these cells was 0.06 μm/second (assessed from Abp1-GFP movements). These data lend further support to the idea that these Sla1p-containing complexes represent a distinct subpopulation of cortical patches in yeast. It was also observed that the patches do not retain the same fluorescence intensity during even these very short time courses. As depicted by the arrows and arrowheads in Fig. 5, some spots decrease in intensity as others are observed to increase. Because the images are 3D images projected onto 2D the decreases and increases in intensity are not simply the spots moving out of focus. Rather this indicates that either the complexes as complete entities are rapidly turned over or that the presence of Sla1p within these complexes is highly dynamic.

Interactions between Sla1p and the endocytic machinery

Tang and colleagues (Tang et al., 2000) used two-hybrid and immunoprecipitation approaches to demonstrate an interaction between the C-terminal repeats of Sla1p and two conserved proteins of the yeast endocytic machinery, End3p and Pan1p. To investigate the importance of this interaction within the cell and the role of the Sla1p C-terminal repeat region further, we first generated a mutant form of Sla1p lacking the entire C-terminal repeat region. This Sla1ΔCt deletion mutant was myc tagged and was shown by western blotting to be expressed at

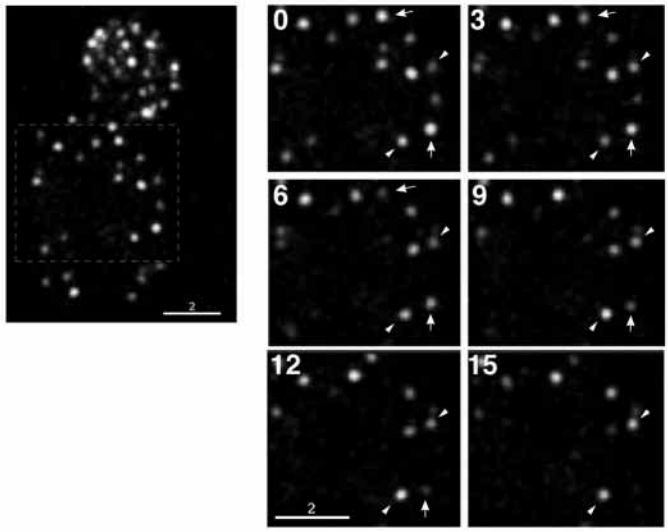

Fig. 5. Localisation of Sla1-GFP in real time. KAY401 cells were taken from a freshly struck YPAD plate and visualised as described in the Materials and Methods. The left panel shows the entire cell (at t=0) from which the subsequent images have been recorded. The images are 2D projections of 3D acquired data (16×0.4 μM optical sections) with 0.02 second exposure, taken every 3 seconds. Arrowheads denote examples of Sla1p-containing spots that remain at the same intensity or increase intensity over this time course. The arrows mark spots that decrease in intensity and disappear completely over the time course. Bar, 2 μm.

similar levels to the wild-type Sla1p. Strains expressing this Sla1ΔCt mutant were able to grow at 37°C, whereas cells that have a complete deletion of *SLA1* cannot grow at this temperature. However, yeast expressing Sla1ΔCt are still dependent on expression of *ABP1* (data not shown). This indicates that the mutant Sla1 protein is produced in these cells and is at least partially functional. The myc-tagged sla1ΔCt protein was then localised using immunofluorescence microscopy. Localisation was compared with a myc-tagged version of the full-length protein. As shown in Fig. 6A, deletion of the C-terminal repeats of Sla1p results in almost complete loss of the protein at the cell cortex. A count of cells revealed that 5% of sla1ΔCt-expressing cells were observed to localise Sla1p to the cortex (n=427) compared with 92% cortical Sla1p localisation in wild-type cells (n=434).

To investigate whether the interactions localising Sla1p to the cell cortex via its C-terminal repeats are mediated through End3p we observed the localisation of Sla1-GFP in wild-type cells and in a strain expressing a temperature-sensitive mutant of End3p (*end3-1*). When this mutant strain is shifted to its non-permissive temperature, the actin cytoskeleton becomes aberrant with cells containing fewer, larger, chunks of actin rather than punctate cortical patches (Benedetti et al., 1994). This actin phenotype is reminiscent of that seen in cells in which *sla1* is deleted (Holtzman et al., 1993). Sla1-GFP localisation was observed in cells at 30°C and then in wild-type and *end3-1* cells following a temperature shift to 37°C for 2 hours. As depicted in Fig. 6B (upper left panels), in the presence of functional End3p, Sla1-GFP localises to discrete cortical spots at both 30°C and at 37°C. However, in the mutant *end3-1* strain, the Sla1-GFP spots are only seen at 30°C (Fig. 6B, upper right panels). A shift to the non-permissive temperature results in a complete loss of Sla1p cortical staining. This loss of localisation is not simply caused by degradation of Sla1p because western blotting of cell extracts reveals that Sla1p levels remain the same after this two hour incubation period. Furthermore, a shift back to the permissive temperature is rapidly followed by Sla1p regaining its normal cortical localisation (data not shown). At the restrictive temperature when Sla1-GFP is cytoplasmically localised, actin organisation observed using rhodamine-phalloidin staining of cells from the same culture is markedly different (Fig, 6C, lower panels). We conclude therefore that End3p must be functional for the correct localisation of Sla1p to the cell cortex and that this mislocalisation of Sla1p might be the cause of the aberrant actin phenotype in the *end3-1* cells. Further evidence for the importance of End3p for Sla1p localisation and for the functionality of the *end3-1* mutant protein at permissive temperatures was gained from the localisation of Sla1-GFP in Δ*end3* cells. Unlike the *end3-1* mutant, these cells show an aberrant 'chunky' actin defect at all temperatures (data not shown), and Sla1-GFP localisation was diffuse in the cell cytosol at all temperatures tested (22-37°C) (Fig. 6D). In some Δ*end3* cells, a number of bright spots of staining can be seen at the cortex, which might indicate that in the absence of any End3p a small proportion of Sla1GFP is able to interact with other proteins such as Pan1p. This, however, appears to be a minor contributor to Sla1p localisation in wild-type cells.

Sla1p plays a role in both fluid-phase endocytosis and internalisation of pheromone receptors

The interaction between Sla1p and End3p indicated that although the most apparent cell phenotypes associated with *SLA1* deletion are on the actin cytoskeleton, there may also be effects on endocytic processes. Initial studies focused on fluid-phase uptake of the dye lucifer yellow that can be seen to accumulate in the vacuoles of wild-type cells following its internalisation (Fig. 7A). This dye is highly soluble and cannot cross biological membranes. Its accumulation in the vacuole therefore depends entirely on endocytic membrane trafficking. In cells in which *sla1* has been deleted, we observed a significant decrease in lucifer yellow uptake (Fig. 7B). Quantitation revealed that only about half of the cells (58%±2) in the Δ*sla1* cell population appeared to endocytose the dye compared with over 90% in the wild-type population. Moreover, in the cells in which vacuolar staining was detected, the intensity of this vacuolar fluorescence was measured and was found to be significantly reduced in the Δ*sla1* cell population, with intensities of 68%±1 of those in wild-type cells. Lucifer yellow uptake was also monitored in cells expressing the C-terminal truncation mutant of Sla1p. These cells showed an almost identical defect in their endocytosis to the Δ*sla1* cells, with 55±2% cells endocytosing the dye and with those showing endocytosis having a reduced intensity of fluorescence in their vacuoles (65±3%) compared with wild-type populations.

Uptake of the dye FM4-64 was also monitored in wild-type and Δ*sla1* cells. This dye can be used to distinguish mutants that have defects in membrane trafficking from those that have defects in the initial internalisation step of endocytosis (Vida and Emr, 1995). Proteins that have strong endocytic defects are

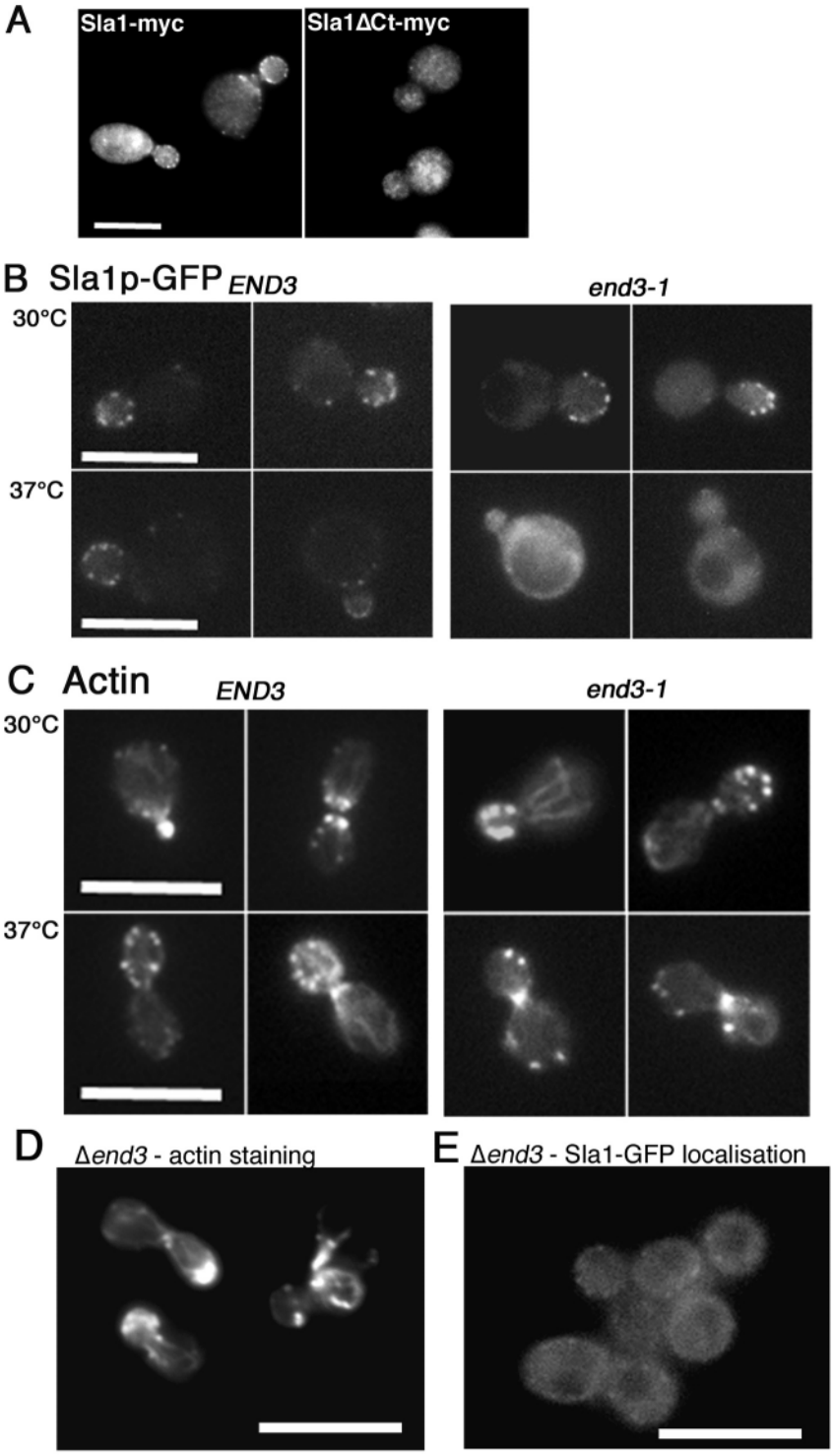

Fig. 6. Interaction of Sla1p at the cell cortex with the endocytic machinery. (A) The effect of deletion of the C-terminal repeat region on Sla1p localisation. Cells expressing full-length 9×myc-tagged Sla1p, KAY303 (left) or mutant sla1ΔCt-9×myc, KAY363 (right) were grown in rich media to log phase and then processed for immunofluorescence as described in the Materials and Methods. Note the lack of cortical localisation of Sla1p in the absence of the C-terminal repeat region. Bar, 10 μM. (B) Localisation of Sla1-GFP in *END3* and *end3*-1 cells following a temperature shift. KAY397 (*END3*) and KAY462 (*end3*-1) cells were grown overnight at 30°C in rich medium to log phase. Half of each culture was then shifted to 37°C, the non-permissive temperature for the *end3*-1 mutation. Cells were incubated at 37°C for 2 hours. Cells were then mounted on slides and images recorded as described in the Materials and Methods. (C) Samples of cells were also taken at this time, fixed and processed for rhodamine-phalloidin staining. Cells showing a complete deletion of *END3* were grown at 30°C and analysed by rhodamine-phalloidin staining to observe their actin phenotype (D) and to assess localisation of Sla1GFP (E). Bar, 10 μM.

still able to transport this dye to the vacuole, although those with defects in trafficking do not. Cells in which *sla1* was deleted showed a slight kinetic delay in FM4-64 uptake, but by 30 minutes labelling was similar to that found in wild-type cells (data not shown).

To assess whether the endocytosis of receptor proteins was also affected by loss of *SLA1* expression, uptake of α-factor pheromone receptor Ste2p was followed using a strain that was characterised previously, in which Ste2p is tagged at its C-terminus with a 9×myc tag (Ayscough and Drubin, 1998b). Localisation of Ste2p was determined by immunofluorescence microscopy following incubation of the cells with α-factor. As reported previously (Ayscough and Drubin, 1998b), in wild-type cells prior to α-factor addition Ste2p localises primarily to the plasma membrane and is seen as a uniform cortical stain (Fig. 8A). It is also found in some internal non-cortical organelles, seen as punctate spots. Shortly after α-factor addition (t=15 minutes) there is a dramatic uptake of the receptor and less than 5% of cells have any cortical staining. After 60 minutes, Ste2p is again observed at the cell surface but now in a polarised organisation. After 120 minutes, this polarised localisation is observed to coincide with the growing mating projection. In the absence of *sla1*, Ste2p is still observed at the cell cortex (Fig. 8B) but very little internalisation is observed following α-factor addition, such that after 15 minutes more than 60% of cells still show cortical staining when assessed by immunofluorescence microscopy. At later time points increased staining is observed at the position of mating projection formation, indicating that new receptor is likely to be secreted in a polarised manner although there is still staining over the entire cortex. These data are summarised graphically in Fig. 8C and indicate that *sla1* deletion causes a significant defect in receptor uptake following pheromone addition.

To address whether the defect observed is at the level of internalisation or at a subsequent stage of membrane trafficking (for example inhibited movement of vesicles away from the membrane), internalisation of radiolabelled pheromone was monitored. Peptide that is bound at the surface

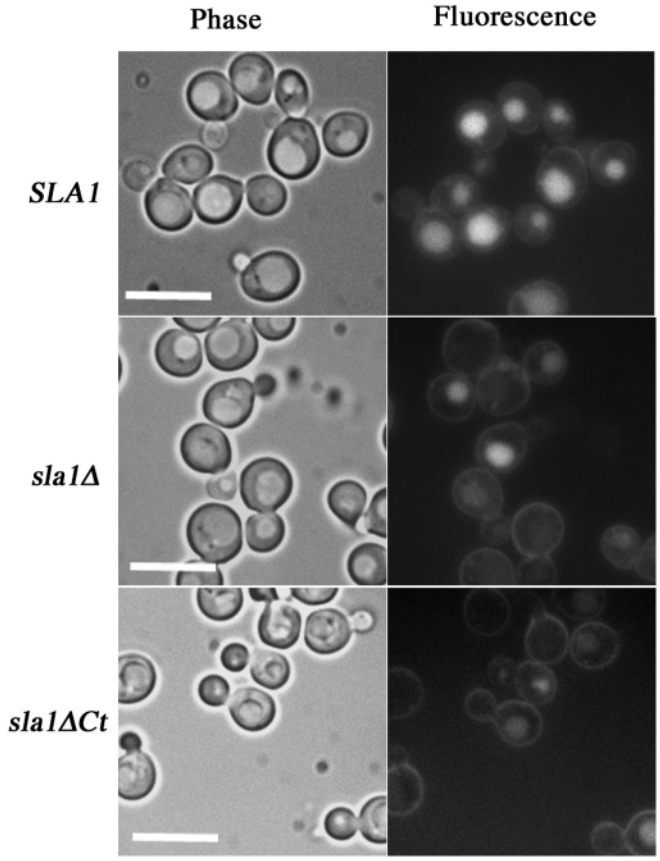

Fig. 7. The effect of deletion and mutation of *SLA1* on fluid-phase endocytosis. Cells in exponential growth phase were incubated with lucifer yellow for 1 hour at room temperature. Vacuole morphology was observed by phase contrast microscopy (left panels) and localisation of lucifer yellow by fluorescence microscopy (right panels). Bar, 10 μM.

but not internalised will be accessible for removal by a harsh pH 1.1 wash (as described). A biologically active but modified form of α-factor was used, which could be iodinated (Siegel et al., 1999) (see Materials and Methods). This radiolabelled peptide called MFN5 was incubated with wild-type and Δ*sla1* cells, and uptake was monitored. As shown in Fig. 8D wild-type cells internalise the pheromone such that an increased level of radiation is associated with the cells. In the absence of Sla1p, the majority of radiation can be washed off the cells indicating that it has not been internalised. This further demonstrates that deletion of *SLA1* causes defects in the initial internalisation step of endocytosis.

Discussion

The importance of the actin cytoskeleton for endocytosis in yeast has been recognised for several years (for a review, see Geli and Riezman, 1998). How the processes are coupled has however remained unclear. The data presented here bring together several lines of evidence and allow us to formulate a model for how Sla1p may play a role in allowing yeast cells to co-ordinate actin dynamics and endocytic events.

The initial identification of Sla1p and its characterisation pointed to a role for this protein in actin organisation and dynamics (Holtzman et al., 1993; Ayscough et al., 1999). Further evidence for this is shown here by the greatly increased latrunculin-A resistance of cells in which *SLA1* has been deleted. Moreover, we have demonstrated that Sla1p can bind to both Abp1p and Las17p/Bee1p, which are two proteins recently shown to enhance actin polymerisation in yeast via interactions with the Arp2/3 complex (Madania et al., 1999; Winter et al., 1999; Goode et al., 2001). In addition, the reported interaction of Pan1p with Sla1p (Tang et al., 2000) and the possible role for Pan1p itself in direct activation of Arp2/3 (Duncan et al., 2001) puts Sla1p in a currently unique position of interacting with all three known Arp2/3 activators in yeast. Having detected in vivo effects on the actin cytoskeleton caused by *sla1* deletion and demonstrated interactions of Sla1p with known regulators of actin in vitro and by immunoprecipitation, it was somewhat surprising to observe a relatively low level of colocalisation between Sla1p and actin-containing complexes. This observation, and evidence emerging from other studies which linked Sla1p to the endocytic proteins End3p and Pan1p (Tang et al., 2000), led us to investigate whether Sla1p might in fact be an adaptor protein coupling proteins of the endocytic machinery to the actin cytoskeleton. Such an interaction might be expected to be regulated and transient, and this would explain the lack of complete colocalisation of Sla1p and actin patches. It is important to note that although some patches contain both Sla1p and Abp1p and other patches contain only one of the proteins, this could be explained in two ways. Firstly, that Sla1p and Abp1p/actin patches pre-exist but become transiently associated in an overlapping complex to regulate certain processes. Secondly, that Sla1p can associate with different cortical complexes, only one of which contains Abp1 and actin. Each patch type would exist and function independently. In the latter case one might predict that Sla1p would associate with different proteins to localise it to the various complexes. This, however, does not appear to be the case because we show that in the absence of a single protein End3p, Sla1p shows no significant cortical localisation (Fig. 7). This result and other data described here lead us to favour the former model that pre-existing complexes become associated in order to link actin dynamics to the process of endocytosis.

The behaviour of Sla1p patches also suggests that they are distinct from the majority of Abp1p/actin patches. Rather than showing rapid cortical movement, most Sla1p patches are relatively static. This might be the behaviour expected of a complex involved in a process such as membrane invagination and endocytosis. It is possible that the actin patches only become associated with this complex transiently and at a certain time in the endocytic process. This may explain, firstly, why not all membrane invaginations appear to be associated with actin (Mulholland et al., 1999) and, secondly, why there are populations of actin patches that are fast moving and others which are almost static. Potentially, it is just the latter that are involved in the endocytic process. Currently, the fluorescent signals from the Sla1-YFP/ Abp1-CFP-expressing strains are not sufficiently robust over time to allow this question to be fully resolved using a FRET approach. Improved strain selection and signal detection may allow this technique to be used successfully in the future. However, using the Sla1-YFP/Abp1-CFP-expressing strains we were able to

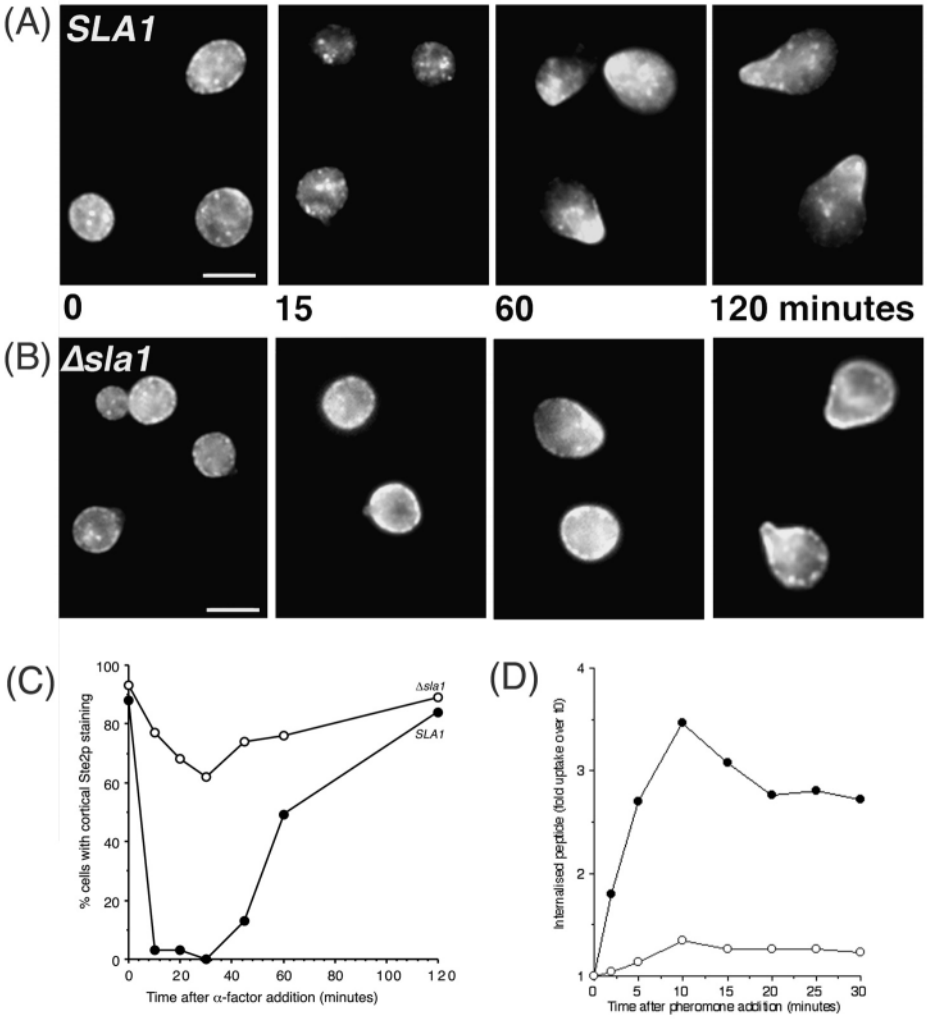

Fig. 8. The effect of deletion of *SLA1* on receptor-mediated endocytosis. (A,B) KAY316 (*SLA1*) and KAY391 (Δ*sla1*) cells were grown to log phase. α-factor (2.5 μg/ml) was added and samples taken and processed for immunofluorescence microscopy at the times indicated. (C) Cells were assessed at each time point for whether the Ste2p-myc staining was at the cortex of cells ($n \geq 200$ for each time point). (D) Uptake of radiolabelled pheromone was monitored in KAY316 and KAY391 strains to further quantify the internalisation defect of Δ*sla1* cells. The graph plotted is the ratio of radioactivity associated with the cells at each time point relative to the initial time zero level of labelling.

demonstrate that despite only a limited amount of colocalisation of Sla1p and Abp1p, when these proteins were in the same complex they are sufficiently close to generate a detectable FRET signal. This supports the idea that Sla1p and Abp1p can interact closely in vivo as well as in vitro and is the first demonstration of such a close interaction between components of the cytoskeleton in live yeast cells. This type of approach will facilitate other investigations of cortical complex association, for example, at specific times in the cell cycle or under conditions such as response to mating pheromone, and may allow us to better dissect the spatial and temporal regulation of the actin cytoskeleton.

The importance of End3p for Sla1p localisation led us to further investigate a role for Sla1p in endocytosis as well as in affecting actin dynamics. End3p has been previously shown to be part of a complex containing Pan1p, the yeast epsin homologue. Deletion of *sla1* causes a significant, though not complete, defect in both fluid-phase and receptor-mediated endocytosis as assessed by a number of approaches. These data demonstrate that the association of Sla1p with the End3p-Pan1p complex is required for normal levels of endocytosis. These results have led us to propose a model in which Sla1p functions to couple endocytic complexes to actin-containing complexes. As outlined in Fig. 9, we envisage Sla1p being localised to a relatively static cortical complex that contains proteins known to be required for endocytosis. Sla1p is able to then mediate an association between this complex and the actin patches through interactions with both Abp1p and Las17/Bee1p. This interaction allows actin polymerisation to take place at specific sites at the cell surface where endocytosis occurs. Possible mechanisms for actin involvement in endocytosis have been recently reviewed (Munn, 2000) and include an actin polymerisation model and a myosin contraction model for driving invagination of endocytic vesicles.

Important ideas as to the factors that regulate association and

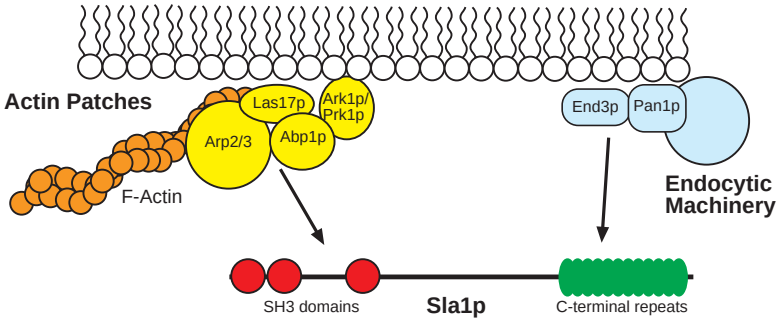

Fig. 9. Model of Sla1p coupling actin dynamics and endocytosis. Our data indicate that in wild-type cells Sla1p is able to interact both with proteins regulating actin dynamics and with proteins forming part of the endocytic machinery. Sla1p localisation at the cell cortex is shown to be largely dependent on the presence of functional End3p, a protein of the endocytic machinery, but a subset of complexes containing Sla1p can also localise with Abp1p-actin structures. We propose that it is in this larger complex that Sla1 binding to Abp1p and Las17p/Bee1p is able to link actin dynamics with the endocytic machinery and thereby facilitate endocytosis.

disassociation of actin patches and endocytic complexes and the mechanistic role that Sla1p plays in the process spring from the findings described here. The C-terminal region of Sla1p contains several motifs, LXXQXTG, that are potential sites of phosphorylation by the actin-regulating kinases Ark1p and Prk1p (Zeng et al., 1999), and this is the domain that is important for Sla1p interaction with End3p (Tang et al., 2000) and which is required for Sla1p cortical localisation (Fig. 6). A recent report shows phosphorylation of Sla1p by Prk1p at its C-terminus (Zeng et al., 2001). Furthermore, Abp1p is reported to bind to Ark1p/Prk1p (Fazi et al., 2001). This suggests a mechanism for regulating association of the complexes such that the kinases are in one complex (Abp1p/actin) and their substrates in a second complex (Sla1p/End3p-Pan1p). Phosphorylation would then occur only after the complexes were brought together and would serve to cause dissociation of this larger complex. A prediction of this model would be that in the absence of Ark1p/Prk1p the endocytic-actin complexes would remain associated. Our unpublished observations indicate that this is the case. Finally, reported interactions between Sla1p and the yeast protein phosphatase-1 Glc7p (Tu et al., 1996; Venturi et al., 2000) may provide a mechanism to reverse the phosphorylation process.

Future studies will now investigate the role that Sla1p plays in augmenting actin dynamics and whether it simply acts as a scaffold to stabilise interactions between a number of other proteins or whether it plays a more active role in actin polymerisation. Our data thus far however support a model in which Sla1p is localised with the endocytic machinery in order to constrain its activity within the cells such that it facilitates actin polymerisation only at appropriate sites on the cell surface.

We are grateful to Steve Winder and Hilary Dewar for critical reading of the manuscript, to Kim Nasmyth, (IMP, Vienna), M. Longtine (University of North Carolina) and the Yeast Resource Center, (University of Washington) for the plasmids used to generate myc and fluorescent-protein-tagged versions of Sla1p and Abp1p, Jamie Cope and David Drubin (UC Berkeley) for the GST-Sla1p plasmids, David Drubin for anti-actin antibodies, B.Winsor (Strasbourg) for anti-Arp2p antibodies and Phil Crews (UC Santa Cruz) for latrunculin-A. This work was supported by a Career Development Fellowship from The Wellcome Trust to K.R.A. (050934/Z/97), BBSRC grant (17/C12769), a BBSRC studentship to D.T.W. and support from the Wellcome Trust to P.D.A. for the Deltavision Microscope facility.

References

Adams, A. E. M. and Pringle, J. R. (1984). Relationship to actin and tubulin distribution to bud growth in wild type and morphogenetic mutant *Saccharomyces cerevisiae*. *J. Cell Biol.* **98**, 934-945.

Ayscough, K. (2000). Endocytosis and the development of cell polarity in yeast require a dynamic F-actin cytoskeleton. *Curr. Biol.* **10**, 1587-1590.

Ayscough, K. R. and Drubin, D. G. (1998a). Immunofluorescence microscopy of yeast cells. In *Cell Biology: A Laboratory Handbook* Vol. 2 (ed. J. Celis), pp. 477-485. New York: Academic Press.

Ayscough, K. R. and Drubin, D. G. (1998b). A role for the yeast actin cytoskeleton in pheromone receptor clustering and signalling. *Curr. Biol.* **8**, 927-930.

Ayscough, K. R., Stryker, J., Pokala, N., Sanders, M., Crews, P. and Drubin, D. G. (1997). High rates of actin filament turnover in budding yeast and roles for actin in establishment and maintenance of cell polarity revealed using the actin inhibitor latrunculin-A. *J. Cell Biol.* **137**, 399-416.

Ayscough, K. R., Eby, J. J., Lila, T., Dewar, H., Kozminski, K. G. and Drubin, D. G. (1999). Sla1p is a functionally modular component of the yeast cortical actin cytoskeleton required for correct localization of both Rho1p-GTPase and Sla2p, a protein with talin homology. *Mol. Biol. Cell* **10**, 1061-1075.

Belmont, L. D. and Drubin, D. G. (1998). The yeast V159N actin mutant reveals roles for actin dynamics in vivo. *J. Cell Biol.* **142**, 1289-1299.

Benedetti, H., Raths, S., Crausaz, F. and Riezman, H. (1994). The *END3* gene encodes a protein that is required for the internalization step of endocytosis and for actin cytoskeleton organization in yeast. *Mol. Biol. Cell* **5**, 1023-1037.

Doyle, T. and Botstein, D. (1996). Movement of yeast cortical actin cytoskeleton visualized *in vivo*. *Proc. Natl. Acad. Sci. USA* **93**, 3886-3891.

Drubin, D. G., Miller, K. G. and Botstein, D. (1988). Yeast actin binding proteins: Evidence for a role in morphogenesis. *J. Cell Biol.* **107**, 2551-2561.

Dulic, V., Egerton, M., Elgundi, I., Raths, S., Singer, B. and Riezman, H. (1991). Yeast endocytosis assays. *Methods Enzymol.* **194**, 697-710.

Duncan, M. C., Cope, M. J., Goode, B. L., Wendland, B. and Drubin, D. G. (2001). Yeast Eps15-like endocytic protein, Pan1p, activates the Arp2/3 complex. *Nat. Cell Biol.* **3**, 687-690.

Fazi, B., Cope, M. T., Douangamath, A., Ferracuti, S., Schirwitz, K., Zucconi, A., Drubin, D. G., Willmanns, M., Cesarini, G. and Castagnoli, L. (2001). Unusual binding propoerties of the SH3 domain of the yeast actin binding protein Abp1: Structural and functional analysis. *J. Biol. Chem.* **277**, 5290-5298.

Geli, M. I. and Riezman, H. (1998). Endocytic internalization in yeast and animal cells: similar and different. *J. Cell Sci.* **111**, 1031-1037.

Goode, B. L., Rodal, A. A., Barnes, G. and Drubin, D. G. (2001). Activation of the Arp2/3 complex by the actin filament binding protein Abp1p. *J. Cell Biol.* **153**, 627-634.

Gordon, G. W., Berry, G., Liang, X. H., Levine, B. and Herman, B. (1998). Quantitative fluorescence resonance energy transfer measurements using fluorescence microscopy. *Biophys. J.* **74**, 2702-2713.

Hagan, I. M. and Ayscough, K. R. (2000). Fluorescence microscopy in yeast. In *Protein Localization by Fluorescence Microscopy: A Practical Approach*. (ed. V. J. Allan), pp. 179-205. Oxford: Oxford University Press.

Holtzman, D. A., Yang, S. and Drubin, D. G. (1993). Synthetic-lethal interactions identify two novel genes, *SLA1* and *SLA2*, that control membrane cytoskeleton assembly in *Saccharomyces cerevisiae*. *J. Cell Biol.* **122**, 635-644.

Kaiser, C., Michaelis, S. and Mitchell, A. (eds) (1994). *Methods in Yeast Genetics: A Laboratory Course Manual*. New York: Cold Spring Harbor Laboratory Press.

Karpova, T. S., Tatchell, K. and Cooper, J. A. (1995). Actin filaments in yeast are unstable in the absence of capping protein. *J. Cell Biol.* **131**, 1483-1493.

Kübler, E. and Riezman, H. (1993). Actin and fimbrin are required for the internalization step of endocytosis in yeast. *EMBO. J.* **12**, 2855-2862.

Li, R. (1997). Bee1, a yeast protein with homology to Wiscott-Aldrich Syndrome Protein, is critical for the assembly of cortical actin cytoskeleton. *J. Cell Biol.* **136**, 649-658.

Lila, T. and Drubin, D. G. (1997). Evidence for physical and functional interactions among two *Saccharomyces cerevisiae* SH3 domain proteins, an adenylyl cyclase-associated protein and the actin cytoskeleton. *Mol. Biol. Cell.* **8**, 367-385.

Longtine, M. S., McKenzie, A., Demarini, D. J., Shah, N. G., Wach, A., Brachat, A., Philippsen, P. and Pringle, J. R. (1998). Additional modules for versatile and economical PCR-based gene deletion and modification in *Saccharomyces cerevisiae*. *Yeast* **14**, 953-961.

Madania, A., Dumoulin, P., Grava, S., Kitamoto, H., Scharer-Brodbeck, C., Soulard, A., Moreau, V. and Winsor, B. (1999). The *Saccharomyces cerevisiae* homologue of human Wiskott-Aldrich syndrome protein Las17p interacts with the Arp2/3 complex. *Mol. Biol. Cell* **10**, 3521-3538.

Morton, W. M., Ayscough, K. R. and McLaughlin, P. J. (2000). Latrunculin alters the actin-monomer subunit interface to prevent polymerization. *Nat. Cell Biol.* **2**, 376-378.

Mulholland, J., Preuss, D., Moon, A., Wong, A., Drubin, D. and Botstein, D. (1994). Ultrastructure of the yeast actin cytoskeleton and its association with the plasma membrane. *J. Cell Biol.* **125**, 381-391.

Mulholland, J., Konopka, J., Singer-Kruger, B., Zerial, M. and Botstein, D. (1999). Visualization of receptor-mediated endocytosis in yeast. *Mol. Biol. Cell* **10**, 799-817.

Munn, A. (2000). The yeast endocytic membrane transport system. *Microsc. Res. Tech.* **51**, 547-562.

Novick, P. and Botstein, D. (1985). Phenotypic analysis of temperature sensitive yeast actin mutants. *Cell* **40**, 405-416.

Olah, M. E., Gallo-Rodriguez, C., Jacobson, K. A., Stiles, G. L. (1994). ^{125}I-4-aminobenzyl-5′-N-methylcarboxamidoadenosine, a high affinity radioligand for the rat A_3 adenosine receptor. *Mol. Pharmacol.* **45**, 978-982.

Raths, S., Rohrer, J., Crausaz, F. and Riezman, H. (1993). end3 and end4: two mutants defective in receptor-mediated endocytosis in *Saccharomyces cerevisiae*. *J. Cell Biol.* **120**, 55-65.

Siegel, E. G., Günther, R., Schäfer, H., Fölsch, U. R. and Schmidt, W. E. (1999). Characterisation of a novel peptide agonists of the α mating factor of *Saccharomyces cerevisiae*. *Anal. Biochem.* **275**, 109-115.

Simon, V. R., Karmon, S. L. and Pon, L. A. (1997). Mitochondrial inheritance: Cell cycle and actin cable dependence of polarized mitochondrial movements in Saccharomyces cerevisiae. *Cell Motil. Cytoskeleton* **37**, 199-210.

Sorger, P. K. and Pelham, H. R. (1987). Purification and characterization of a heat-shock element binding protein from yeast. *EMBO J.* **6**, 3035-3041.

Sorkin, A., McClure, M., Huang, F. T. and Carter, R. (2000). Interaction of EGF receptor and Grb2 in living cells visualized by fluorescence resonance energy transfer (FRET) microscopy. *Curr. Biol.* **10**, 1395-1398.

Tang, H. and Cai, M. (1996). The EH-domain containing protein Pan1 is required for normal organization of the actin cytoskeleton in *Saccharomyces cerevisiae*. *Mol. Cell. Biol.* **16**, 4897-4914.

Tang, H. Y., Munn, A. and Cai, M. J. (1997). EH domain proteins Pan1p and End3p are components of a complex that plays a dual role in organization of the cortical actin cytoskeleton and endocytosis in Saccharomyces cerevisiae. *Mol. Cell. Biol.* **17**, 4294-4304.

Tang, H. Y., Xu, J. and Cai, M. J. (2000). Pan1p, End3p, and Sla1p, three yeast proteins required for normal cortical actin cytoskeleton organization, associate with each other and play essential roles in cell wall morphogenesis. *Mol. Cell. Biol.* **20**, 12-25.

Tebar, F., Sorkina, T., Sorkin, A., Ericsson, M. and Kirchausen, T. (1996). Eps15 is a component of clathrin-coated pits and vesicles and is located at the rim of coated pits. *J. Biol. Chem.* **271**, 28727-28730.

Tu, J. L., Song, W. J. and Carlson, M. (1996). Protein phosphatase type 1 interacts with proteins required for meiosis and other cellular processes in *Saccharomyces cerevisiae*. *Mol. Cell. Biol.* **16**, 4199-4206.

Venturi, G. M., Bloecher, A., Williams-Hart, T. and Tatchell, K. (2000). Genetic interactions between GLC7, PPZ1 and PPZ2 in *Saccharomyces cerevisiae*. *Genetics* **155**, 69-83.

Vida, T. A. and Emr, S. D. (1995). A new vital dye for visualising vacuolar membrane dynamics and endocytosis in yeast. *J. Cell Biol.* **128**, 779-792.

Waddle, J., Karpova, T., Waterson, R. and Cooper, J. (1996). Movement of cortical actin patches in yeast. *J. Cell Biol.* **132**, 861-870.

Wendland, B. and Emr, S. D. (1998). Pan1p, yeast eps15, functions as a multivalent adaptor that coordinates protein-protein interactions essential for endocytosis. *J. Cell Biol.* **141**, 71-84.

Wesp, A., Hicke, L., Palecek, J., Lombardi, R., Aust, T., Munn, A. L. and Riezman, H. (1997). End4p/Sla2p interacts with actin-associated proteins for endocytosis in *Saccharomyces cerevisiae*. *Mol. Biol. Cell* **8**, 2291-2306.

Winter, D., Lechler, T. and Li, R. (1999). Activation of the yeast Arp2/3 complex by Bee1p, a WASP-family protein. *Curr. Biol.* **9**, 501-504.

Zeng, G. S. and Cai, M. J. (1999). Regulation of the actin cytoskeleton organization in yeast by a novel serine/threonine kinase Prk1p. *J. Cell Biol.* **144**, 71-82.

Zeng, G. S., Yu, X. and Cai, M. J. (2001). Regulation of the yeast actin cytoskeleton-regulatory complex Pan1p/Sla1p/End3p by serine/threonine kinase Prk1p. *Mol. Biol. Cell* **12**, 3759-3773.